

Enhanced mechanical properties of 1,3-trimethylene carbonate polymers and networks

Ana Paula Pêgo, Dirk W. Grijpma, Jan Feijen*

Institute for Biomedical Technology (BMTI), Faculty of Chemical Technology, Department of Polymer Chemistry and Biomaterials, University of Twente, P.O. Box 217, 7500 AE Enschede, The Netherlands

Received 14 March 2003; accepted 1 July 2003

Abstract

Poly(1,3-trimethylene carbonate), poly(TMC), has often been regarded as a rubbery polymer that cannot be applied in the biomedical field due to its poor dimensional stability, tackiness and inadequate mechanical properties. In this study we show that high molecular weight, amorphous poly(TMC) is very flexible, tough and has excellent ultimate mechanical properties. A number average molecular weight (\bar{M}_n) of 100,000 was determined to be a critical value below which the polymer has negligible mechanical properties and poor dimensional stability. This corresponds to a molecular weight that is 40 times higher than the molecular weight between entanglements. The dependency of the mechanical properties levels off at \bar{M}_n values above 200,000. This very high molecular weight poly(TMC) shows good recovery after mechanical deformation, considering that the only resistance to chain flow is due to chain entanglement. Poly(TMC) cross-linked upon gamma-irradiation, resulting in the formation of an insoluble network. The degree of cross-linking increases with the radiation dose. The final mechanical properties of the high molecular weight poly(TMC) rubbers improve upon irradiation. Especially, the creep resistance increased, while the Young's modulus and tensile strength were not significantly affected. These biodegradable cross-linked rubbers may find wide application in soft tissue engineering where tough and elastomeric scaffolds are desirable.

© 2003 Elsevier Ltd. All rights reserved.

Keywords: Cross-linking; Elastomeric; Gamma irradiation

1. Introduction

The need for biodegradable elastomeric polymers for the preparation of medical implants and porous scaffolds to be used for tissue engineering has been documented in literature in recent years [1–3]. The traditionally used glycolide and lactide based (co)polymers are not well suited for the preparation of soft tissue implants. These materials are rigid as their glass transition temperature (T_g) is above body temperature [4].

For soft tissue engineering, the matrices and scaffolds on which seeded cells organize and develop into a desired tissue in vitro and/or in vivo would ideally be made of biodegradable polymers of which the properties resemble those of the extracellular matrix (ECM). Elastomeric porous structures, which adjust to the dynamics of the surrounding and developing tissue and provide adequate micro-stresses

to the cells as well as ensure mechanical stability and structural integrity to the developing tissue, are therefore desirable.

Biodegradable elastomeric materials that have previously been investigated include copolymers of lactide (LA) and ϵ -caprolactone (CL) [5], poly-4-hydroxybutyrate [6], and poly(glycerol-sebacate) networks [3]. Homopolymeric 1,3-trimethylene carbonate (TMC), an elastomeric aliphatic polycarbonate, has long been known [7] and its suitability for the preparation of biomedical implants has been previously evaluated [8]. Poly(TMC) used in those studies had a very low modulus and low tensile strength. These poor mechanical properties discouraged any practical application, other than the use of TMC as a softening unit in copolymers or poly(TMC) blends with high modulus polymers [9,10]. Furthermore, TMC based copolymers and poly(TMC) blends were used as matrices for controlled drug release [11–13].

We recently reported [14] that very high molecular weight amorphous poly(TMC) ($\bar{M}_n = 290,000$ and

* Corresponding author. Tel.: +31-53-489-2976; fax: +31-53-489-3823.
E-mail address: j.feijen@ct.utwente.nl (J. Feijen).

$\bar{M}_w = 552,000$), is very flexible and tough with excellent ultimate mechanical properties due to strain-induced crystallization ($T_m = 36^\circ\text{C}$). This self-reinforcement, also observed for natural rubber, is the origin of the high tensile strength and maximal extensibility of this strain-crystallizable physical network [15]. In addition, high molecular weight poly(TMC) was found to be totally resorbed after 3 weeks of subcutaneous implantation in rats. The degradation and resorption of the polymer induced only a mild tissue reaction [16].

In this paper, the influence of the molecular weight of poly(TMC) on its mechanical properties is addressed. The stress–strain behavior in cyclic loading and the creep behavior of high molecular weight poly(TMC) were determined to get insight in the performance of this polymer in a dynamic environment. Finally, in view of the possible use of implants based on poly(TMC) in the clinic, the possibility to sterilize the scaffolds by means of a standard sterilization method was studied. Poly(TMC) films were sterilized by gamma-radiation and analyzed for changes in physical and mechanical properties.

2. Materials and methods

2.1. Materials

Polymer grade 1,3-trimethylene carbonate (TMC) was obtained from Boehringer Ingelheim, Germany and used without further purification. Hexanol (Merck, Germany) was distilled from CaH_2 (Acros, Belgium). Stannous octoate (SnOct_2) (stannous 2-ethylhexanoate) was used as received from Sigma, USA. Solvents (Biosolve, The Netherlands) were of analytical grade.

2.2. Polymer synthesis

In an argon atmosphere, TMC monomer was charged into freshly silanized (Serva, Boehringer Ingelheim Bio-products Partnership, Germany) and dried glass ampoules and 2×10^{-4} mol of stannous octoate per mol of monomer was added as a solution in sodium-dried pentane. The pentane was removed afterwards by evacuation. The ampoules were purged three times with dry argon and heat-sealed under vacuum. Several poly(TMC) batches were prepared (Table 1). For batches 1 and 2, 2×10^{-5} mol of hexanol per mol of monomer was added prior to the purging step. In this case purging was performed after cooling of the ampoules with liquid nitrogen to prevent evaporation of the hexanol (initiator). By exposing the monomer to air for different periods of time, the purity of the monomer can be decreased in a more or less controlled manner. In this way very high molecular poly(TMC) of differing molecular weights could be prepared. For batches 3–8, the monomer was exposed to air for a period of time up to 120 min. The ampoules were conditioned in an oil bath

Table 1
Characteristics of the TMC homopolymers after purification

Sample	$\bar{M}_n \times 10^{-5}$	$\bar{M}_w \times 10^{-5}$	PDI	$[\eta]^a$ (dl/g)	T_g ($^\circ\text{C}$)
Poly(TMC) ₁	0.57	0.92	1.62	1.19	–19
Poly(TMC) ₂	1.09	1.85	1.70	1.79	–18
Poly(TMC) ₃	2.72	5.38	1.98	4.51	–19
Poly(TMC) ₄	3.06	5.30	1.73	4.29	–17
Poly(TMC) ₅	3.27	4.82	1.47	4.20	–19
Poly(TMC) ₆	3.33	5.83	1.75	4.52	–17
Poly(TMC) ₇	3.37	5.59	1.67	4.49	–17
Poly(TMC) ₈	3.55	6.17	1.74	4.85	–18

^a In CHCl_3 , 25°C .

pre-heated to the polymerization temperature and vigorously shaken in order to obtain a homogeneous mixture of the monomers and the catalyst. Polymerizations were carried out for a period of 2 h (batch 1), 3 h (batch 2) or 3 days at $130 \pm 2^\circ\text{C}$. After the selected reaction time the ampoules were quenched to room temperature and the polymers were discharged. The polymers were purified by dissolution in chloroform (2–5 wt/vol.% solutions), filtration of the solutions through a sintered glass filter and precipitation into a 10-fold volume of methanol. Subsequently the polymers were collected, washed with fresh methanol and dried under reduced pressure at room temperature until constant weight.

2.3. Polymer processing

Compression molding of purified polymers was done on a Fontijne laboratory press THB008 (The Netherlands) in 600 μm thick stainless steel molds. The films were melt-pressed at 140°C and subsequently cooled to 15°C under pressure.

2.4. Polymer characterization

2.4.1. Gel permeation chromatography (GPC)

Weight and number average molecular weight (\bar{M}_w and \bar{M}_n , respectively), polydispersity index (PDI) and intrinsic viscosity ($[\eta]$) were determined by GPC using a Waters Model 510 pump (USA), a HP Ti-Series 1050 autosampler (USA), a Waters Model 410 Differential Refractometer and a Viscotek H502 Viscometer Detector (USA) with Waters Styragel HR5-HR4-HR2-HR1 columns placed in series. Chloroform was used as an eluent at a flow rate of 1.5 ml/min. Narrow polystyrene standards were used for calibration. Sample concentrations of approximately 0.5 wt/vol.% and injection volumes of 30 μl were used. All determinations were performed at 25°C .

2.4.2. Differential scanning calorimetry (DSC)

The thermal properties of the purified samples were evaluated by DSC. Samples (5–15 mg) placed in aluminum pans were analyzed with a Perkin–Elmer Pyris1 (USA) at a heating rate of $10^\circ\text{C}/\text{min}$. All samples were heated to 40°C

above their glass transition temperature. Subsequently, the samples were quenched rapidly (300 °C/min) until 40 °C below their glass transition temperature and after 5 min a second scan was recorded. Unless mentioned otherwise, the data presented were collected during the second heating scan. The glass transition temperature (T_g) was taken as the midpoint of the heat capacity change and the peak melting temperature (T_m) was determined from the melting endotherm. Indium, gallium and tin were used as standards for temperature calibration.

2.4.3. Density

The density of poly(TMC) was determined by measuring the dimensions and the mass of melt-pressed polymer films (poly(TMC)₆). The density of poly(TMC) is 1.31 g/cm³.

2.5. Mechanical properties

All mechanical tests were performed in triplicate on compression-molded films with dimensions in accordance to ASTM standard D882-91 specifications (100 × 5 × 0.6 mm³). The mechanical tests were carried out on a Zwick Z020 universal tensile testing machine (Germany) at room temperature (18–20 °C).

2.5.1. Tensile testing

Tensile tests were carried out on the tensile testing machine equipped with a 500 N load cell, operated at a crosshead speed of 50 mm/min. The specimen deformation was derived from the grip-to-grip separation, the initial grip-to-grip separation being 50 mm.

2.5.2. Cyclic loading

Cyclic tests were carried out on the tensile testing machine equipped with a 10 N load cell, operated at a crosshead speed of 50 mm/min. The specimen deformation was derived from the grip-to-grip separation, the initial grip-to-grip separation being 50 mm. The films were deformed cyclically (20 cycles) up to 50% strain. The 21st cycle was started after a 2-h recovery period.

2.5.3. Creep

For the creep experiments the tensile testing machine was equipped with a 10 N load cell. The specimen deformation was derived from the grip-to-grip separation, the starting grip-to-grip separation being 50 mm. The samples were stressed to 0.1, 0.2, 0.4 and 0.6 N/mm² and the strain was measured as a function of time during 1 h.

2.6. Wide angle X-ray scattering

X-ray diffraction data of compression molded poly(TMC), films were collected on a Philips PW3710 based X'Pert-1 diffractometer (The Netherlands) in Bragg-Brentano geometry, using Cu K α radiation and a θ compensating divergence slit. Data collection was per-

formed at room temperature, using a low-background spinning specimen holder. The measured diffractograms were converted to fixed slit intensities. The peak positions were extracted using the pattern decomposition program PROFIT. The observed individual lines and clusters of lines were fitted using Pearson VII functions, taking the K α ₂ component into account. The obtained peak positions and relative intensities are, therefore, extracted from the analytical K α ₁ peak profiles. The absolute, relative and integral intensities are based on peak heights or areas, respectively, using a θ compensating divergence slit, or, when using the back-calculated diffractograms, on a fixed slit width.

2.7. Plateau modulus determinations in the melt

The cross-over modulus (G_c , where $G'(\omega) = G''(\omega)$) of a poly(TMC) melt was measured by dynamic oscillation using parallel plates on a Universal Dynamic Spectrometer (Physica UDS200, Paar Physica, USA) at 195 °C. The frequency sweeps were performed at 1% strain. From this the plateau modulus (G_n^0) can be calculated, using the polydispersity index (PDI) of the polymer post testing, according to the following relationship [17]:

$$\log\left(\frac{G_n^0}{G_c}\right) = 0.38 + \frac{2.63 \log(\text{PDI})}{1 + 2.45 \log(\text{PDI})} \quad (1)$$

Calculation of the molecular weight between entanglements (M_e) proceeds according to Eq. (2): [18]

$$M_e = \frac{\rho RT}{G_n^0} \quad (2)$$

where ρ is the density of the polymer, T is the temperature and R is the gas constant. Samples for dynamic oscillation measurements were punched out ($\phi = 26$ mm) from compression molded films of purified polymer (poly(TMC)₇) with a thickness of 600 μm .

2.8. Gamma-irradiation

Poly(TMC)₃ samples (in triplicate) were placed in poly(ethylene)/poly(amide) bags and sealed after evacuation. The samples were exposed to 15, 25 and 40 kGy gamma-irradiation from a ⁶⁰Co source (Gammaster, Ede, The Netherlands). In another experiment poly(TMC) films (poly(TMC)₅) were packed under vacuum, in N₂ or in air and were exposed to 25 kGy gamma-irradiation from a ⁶⁰Co source.

Equilibrium swelling experiments (in triplicate) were performed at room temperature using chloroform. The samples were swollen for 1 week to reach equilibrium and subsequently the extracted gels were dried under vacuum at room temperature for 2 weeks until constant weight. The gel and the sol fractions of the irradiated samples were

calculated according to Eqs. (3) and (4), respectively:

$$\text{gelfraction} = \frac{m_d}{m_i} \quad (3)$$

$$\text{solfraction} = 1 - \frac{m_d}{m_i} \quad (4)$$

where m_d is the mass of the extracted and dried gels and m_i is the mass of the specimens before swelling and extraction. The degree of swelling (q) was calculated from the ratio of the weight of swollen and extracted samples (m_s) and the dried gels (m_d) and the specific densities of solvent (ρ_s) (1.4832 g/cm³ for chloroform [19]) and poly(TMC) ($\rho = 1.31$ g/cm³) using:

$$q = 1 + \rho \left(\frac{m_s}{m_d \rho_s} - \frac{1}{\rho_s} \right) \quad (5)$$

3. Results and discussion

3.1. Polymer synthesis and characterization

Until now in studies dealing with the determination of the mechanical properties of poly(TMC), polymer with a relatively low molecular weight was used ($\bar{M}_n < 55,000$ or $[\eta] < 1.7$ dl/g in CHCl₃ at 25 °C) [1,8,20]. Previously, we have seen that strain-induced crystallization occurred upon stretching of poly(TMC) samples of high molecular weight ($\bar{M}_n = 290,000$ and $\bar{M}_w = 552,000$) [14]. In order to evaluate the effect of the molecular weight on the mechanical properties of poly(TMC) a number of polymers covering a broad range of molecular weights was synthesized by ring-opening polymerization in the melt, using stannous octoate as a catalyst/initiator. An overview of the properties of purified TMC polymers is given in Table 1.

In polymerizations with SnOct₂ the initiating species are formed in situ as a result of the reaction of 'hydroxyl' containing impurities present in the polymerization atmosphere, the monomer, or the SnOct₂ catalyst [21]. Poly(TMC) specimens with different molecular weights were obtained by the addition of hexanol to the reaction mixture as a co-initiator (specimens 1 and 2) or by exposing the monomer to air for different time periods prior to polymerization (specimens 3–8).

Mark-Houwink coefficients for poly(TMC) in chloroform were determined by plotting $\log[\eta]$ against $\log \bar{M}_w$ derived from the GPC measurements. Linear fitting of the data ($r = 0.994$) gave values of $K = 2.43 \times 10^{-4}$ and $a = 0.74$, in good agreement with previously reported results [20] for lower molecular weight polymers.

All polymers were amorphous and in the rubbery state at room temperature.

3.2. Effect of poly(TMC) molecular weight on stress–strain behavior

Transparent films could readily be obtained by compression molding. Films prepared from poly(TMC)₁ and poly(TMC)₂ were not dimensionally stable and had the tendency to stick together when pressed against each other. Films prepared from the other batches maintained their initial dimensions even when incubated under physiological conditions (in phosphate buffered saline, at 37 °C) for long periods of time [22] or when implanted in vivo [16], as shown in previous studies.

The mechanical properties of the prepared TMC polymers are listed in Table 2. The \bar{M}_w , \bar{M}_n and $[\eta]$ of the polymers after compression molding are also given. Independent of the initial molecular weight, thermal processing of the purified polymers did not result in extensive chain scission.

Typical stress–strain curves are presented in Fig. 1. The polymer with the lowest molecular weight ($\bar{M}_n = 53,000$) has the lowest modulus, and lowest tensile strength. Poly(TMC)₂ has a higher Young's modulus and a very high ultimate tensile strain, but is also very weak, having a tensile strength of approximately 1 MPa and deforming irreversibly at very low stresses. Polymers with a \bar{M}_n above 200,000 have a higher modulus and a higher strain at yield. The Young's modulus, the yield stress and the maximum tensile strength do not change with molecular weight above \bar{M}_n values higher than 200,000 (Fig. 2(A)–(C), respectively). An upturn in the stress–strain curve at high elongations was only observed for the very high molecular weight ($\bar{M}_n > 200,000$) polymers. Upon fracture and release of the applied force in the tensile testing experiments, the specimens did not recoil.

The thermal behavior of sections of the drawn specimens was analyzed by DSC. With the exception of poly(TMC)₁ samples, which had the lowest \bar{M}_n , the initially amorphous

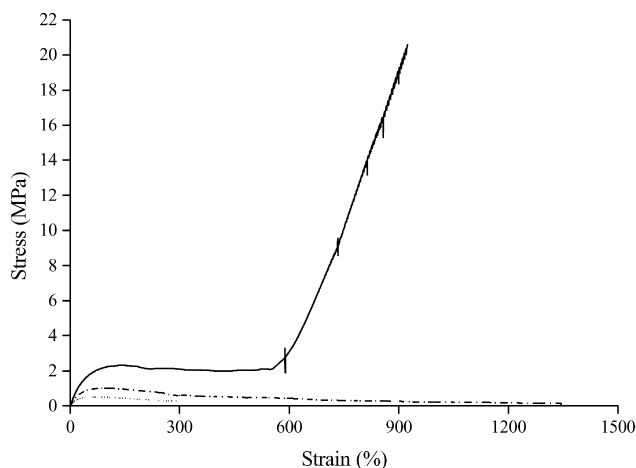


Fig. 1. Stress–strain curves of TMC homopolymers with different molecular weights. (···) Poly(TMC)₁, $\bar{M}_n = 53,000$; (---) poly(TMC)₂, $\bar{M}_n = 94,000$ and (—) poly(TMC)₆, $\bar{M}_n = 273,000$.

Table 2
Molecular weights and stress–strain behavior of compression molded poly(TMC) films

TMC content (mol%)	$\bar{M}_n \times 10^{-5}$	$\bar{M}_w \times 10^{-5}$	$[\eta]$ (dl/g)	Young's modulus (MPa)	σ_{yield} (MPa)	$\varepsilon_{\text{yield}}$ (%)	σ_{break} (MPa)	$\varepsilon_{\text{break}}$ (%)	σ_{max} (MPa)
Poly(TMC) ₁	0.53	0.88	1.16	3.0	0.5	63	0.2	230	0.5
Poly(TMC) ₂	0.94	1.68	1.81	4.7	1.1	98	0.2	1250	1.1
Poly(TMC) ₃	2.08	5.26	4.15	–	–	–	–	–	–
Poly(TMC) ₄	2.23	5.07	4.21	6.6	2.1	120	15	890	16
Poly(TMC) ₅	2.75	5.15	3.86	–	–	–	–	–	–
Poly(TMC) ₆	2.73	5.63	4.59	6.2	2.3	140	16	850	16
Poly(TMC) ₇	3.37	5.83	4.34	6.3	2.3	130	12 ^a	830 ^a	12 ^a
Poly(TMC) ₈	2.21	5.74	4.83	6.8	2.3	150	17	830	17

^a Specimen slipped from grips.

poly(TMC) specimens now showed a melting endotherm with a peak melting temperature (T_m) that ranged between 30 and 50 °C. The DSC scans for one of these samples, before and after tensile testing, are shown in an earlier publication [14]. These findings confirm that the increase in the stress at break found for these polymers results from strain-induced crystallization. In Fig. 3 the tensile strength for each polymer is plotted as a function of the heat of fusion of the strained specimens. A higher crystallinity of the polymer resulted in a higher tensile strength.

Wide angle X-ray scattering (WAXS) measurements performed on a completely amorphous poly(TMC) film and on the same specimen after crystallization upon stretching, confirmed the results of the thermal analyses. In the amorphous state two broad peaks were detected with maxima at $2\theta = 21.2$ and 41.8° . After straining to 850%, the level of order of the polymer chains increased, as can be seen from the WAXS pattern shown in Fig. 4. The X-ray scan of the sample after tensile testing shows distinct and narrower peaks at 2θ values of 20.2, 21.4, 25.8 and 31.2° .

The crystallinity (x_c) of the drawn sample was determined by comparison of the area under the peaks corresponding to the scattering intensities of the amorphous (I_a) and crystalline (I_c) fractions, according to the expression [23]:

$$x_c = \frac{I_c}{I_c + I_a} \quad (6)$$

The contribution of the crystalline fraction to the scattering was determined after deconvolution of the peak signals. For this the WAXS pattern of the amorphous sample was taken into consideration (Fig. 4). A degree of crystallinity of 31% was calculated as described above, corresponding to a ΔH of 27 J/g as determined by DSC. Assuming proportionality of the degree of crystallinity and the experimental ΔH , the heat of fusion of 100% poly(TMC) (ΔH°) can then be estimated to be 87 J/g. It should be noticed that this value is only a rough estimation [23] and should be validated by other methods to determine crystallinity such as based on the densities of the crystalline and amorphous polymer [24]. The crystal structure of (oriented) poly(TMC) then needs to be determined from WAXS measurements. This is beyond the scope of this study.

From the dependency of the mechanical properties on molecular weight it can be concluded that for poly(TMC) an \bar{M}_n of 100,000 is a characteristic minimum molecular weight [25] below which the tensile strength is still typical for a low molecular weight material. Above this value the tensile strength increases significantly with increasing molecular weight. For \bar{M}_n values above 200,000 the change in tensile strength as well as in the other measured mechanical properties levels off. Low molecular weight poly(TMC) possesses a high number of chain ends per unit volume which reduce the packing efficiency of the polymer chains preventing crystallization. With an increase in molecular weight, a higher percentage of the structure can be permanently oriented by stretching, resulting in a higher ultimate tensile strength [26].

The tensile strength of amorphous polymers is influenced by the density of chain entanglements. Amorphous polymers above the glass transition temperature only have any appreciable strength when their molecular weight is at least 2–4 times higher than the molecular weight between entanglements (M_e) [25,27,28]. In the polymer melt, the value of M_e is determined by the intrinsic stiffness of the polymer chain. Estimations of the M_e in the melt can be obtained from determination of the cross-over modulus of the polymer melt in dynamic oscillation. The cross-over modulus (where $G' = G''$, see Fig. 5) was determined to be 2.4×10^5 Pa.

Considering that the PDI of the poly(TMC) sample after the test was 2.40 ($\bar{M}_n = 2.1 \times 10^5$ and $[\eta] = 3.8$), the plateau modulus (G_n^0) was estimated to be approximately 1.9×10^6 Pa. Using the measured density of 1.31 g/cm^3 , for poly(TMC) at 195 °C the value for the molecular weight between entanglements was calculated to be 2700. This shows that in the melt the entanglement density of poly(TMC) is high. Surprisingly, a molecular weight that is at least 40 times higher than this M_e is required for the polymer to show appreciable mechanical properties.

3.3. Stress–strain behavior in cyclic loading and creep behavior of poly(TMC)

To be of practical use in the preparation of medical implants or scaffolds for tissue engineering that will be used

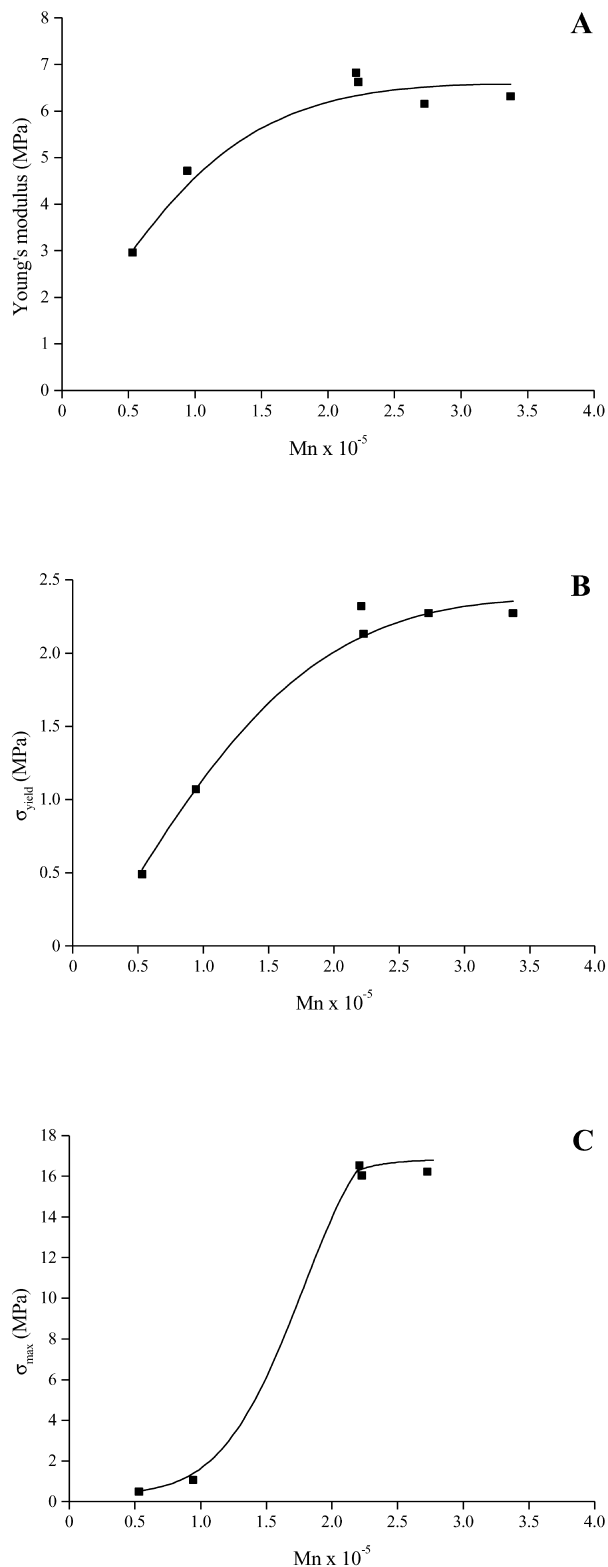


Fig. 2. Young's modulus, stress at yield (σ_{yield}) and maximum tensile strength (σ_{max}) as a function of the number average molecular weight (\bar{M}_n) of poly(TMC).

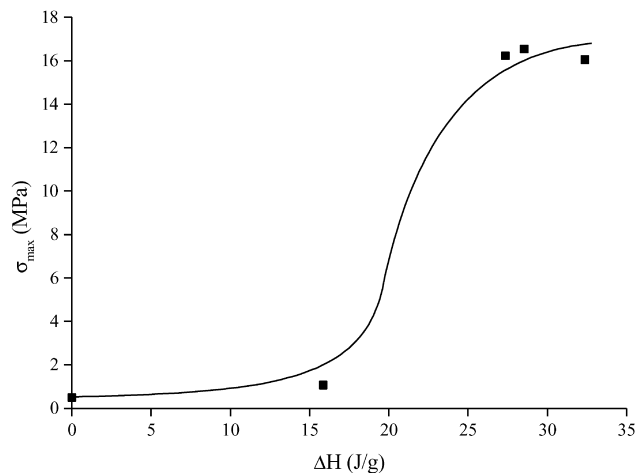


Fig. 3. Maximum tensile strength (σ_{max}) of the TMC homopolymers as a function of the heat of fusion (ΔH) of the specimens after tensile testing.

in the body, poly(TMC) must sustain and recover from repeatedly applied stresses and strains.

In order to evaluate the behavior of high molecular weight poly(TMC) under cyclic loading, polymer films were deformed cyclically up to 50% strain. After 20 cycles a 2-h recovery period was allowed and subsequently a last cycle was recorded. In Fig. 6 the typical stress–strain curves recorded for the different loading cycles are presented.

At the beginning of the 21st cycle the permanent set was determined. This permanent deformation is an important parameter as it can be directly related to the hysteresis phenomenon [29]. For high molecular weight poly(TMC) a permanent set of 4.6% was found after 2 h. For an ideal elastomer, plastic deformation is absent and the permanent set is zero.

The creep behavior of a polymer is another phenomenon resulting from viscous flow. Creep can be defined as a progressive increase in strain over an extended period of time in a polymer subjected to a constant stress.

Creep curves were obtained by applying a constant stress to poly(TMC) films during 1 h and monitoring the strain as a

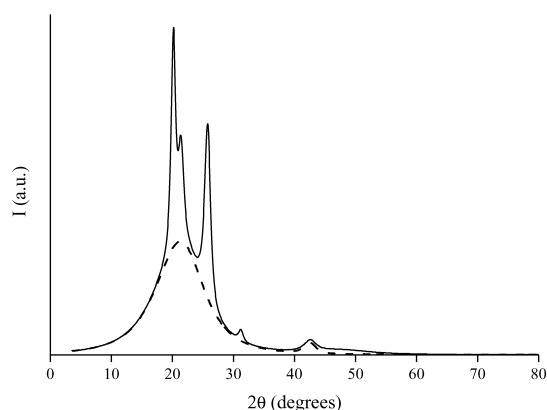


Fig. 4. WAXS pattern of a poly(TMC)₆ film after tensile testing (solid line). The area under the dotted line corresponds to the scattering intensity of the amorphous fraction (I_a).

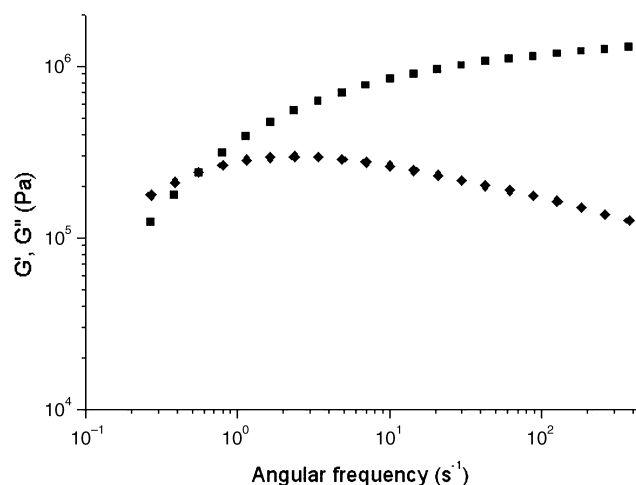


Fig. 5. Linear viscoelastic G' (■) and G'' (◆) master curves at 195 °C for poly(TMC) (poly(TMC)₇ compression molded films).

function of time. The applied stresses corresponded to 5–30% of the yield stress measured by conventional tensile testing. A typical creep curve obtained in this way consisted of an initial elastic response where the elongation of the tensile stress is inversely proportional to the modulus of the material. This was followed by a stage of primary creep, where the creep rate decreases in time and a secondary creep stage, characterized by a constant creep rate. The creep behavior of poly(TMC) films was expressed in terms of the constant creep rate (ASTM standard D2990). The results obtained are summarized in Table 3.

As can be expected the constant creep rate increased with the increase of the applied stress. At 30% of the yield stress the constant deformation rate is substantially higher than at lower stresses. Although poly(TMC) scaffolds to be used in soft tissue engineering will not be subjected to severe load bearing conditions, they will be subjected to some stresses for long periods of time, therefore the creep behavior of the polymer should be taken into account.

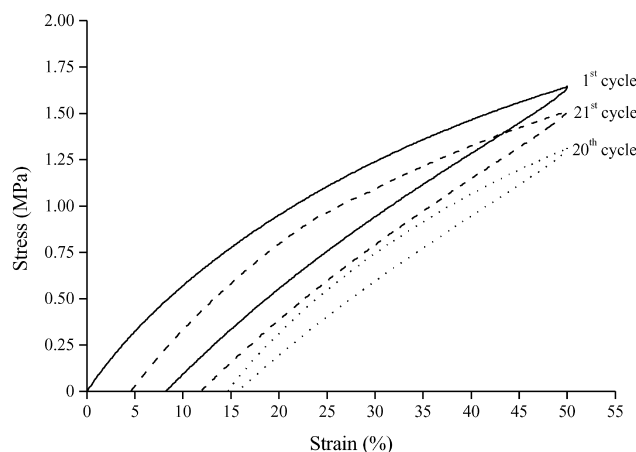


Fig. 6. Cyclic tensile test for high molecular weight poly(TMC)₃ compression molded films.

Table 3

Creep behavior of high molecular weight poly(TMC)

Applied stress (MPa)	Creep rate (s ⁻¹)
0.1 (5%) ^a	1.9×10^{-5}
0.2 (10%)	2.4×10^{-5}
0.4 (20%)	3.8×10^{-5}
0.6 (30%)	12.5×10^{-5}

Poly(TMC)₅ compression molded films.

^a The values in brackets correspond to approximate percentages of the yield stress in tensile tests.

3.4. Gamma-irradiation

The possibility of sterilization of a polymer is a sine qua non for its application in the preparation of implantable medical devices. We investigated the possibility of using ⁶⁰Co gamma-radiation sterilization, as it has the advantages of high efficiency, negligible thermal effects and does not involve the use of toxic substances [30]. In order to evaluate the effect of gamma-radiation on the mechanical properties of poly(TMC), high molecular weight polymer films (packed under vacuum) were exposed to different radiation doses, including 25 kGy, the standard radiation dose for the sterilization of medical devices [30].

Unexpectedly [31], after irradiation at average radiation doses of 15, 25 or 40 kGy, the specimens were not soluble anymore in chloroform. Instead a gel was obtained indicating that poly(TMC) had cross-linked upon radiation. Table 4 presents the degree of swelling of the formed gels as well as the gel fraction of irradiated samples.

Consistent with a decrease in the degree of swelling, the gel fraction of the samples increased with radiation dose, indicating an increase in cross-linking density with radiation dose.

Cross-linking and/or chain scission are known to occur in polymers when these are exposed to high-energy radiation. For most polymers either cross-linking or chain scission prevails [32–34]. In order to investigate the behavior of poly(TMC) the obtained results were analyzed in terms of the Charlesby-Pinner equation [35], which relates the sol fraction (s) of the irradiated samples to the radiation dose (r , expressed in Mrad):

$$s + \sqrt{s} = \frac{G(s)}{2G(x)} + \frac{1}{2.08 \times 10^{-6} G(x) \bar{M}_n r} \quad (7)$$

where, $G(s)$ is the number of main-chain scissions and $G(x)$ the number of cross-links, both produced per 100 eV

Table 4

Degree of swelling and gel fraction of poly(TMC)₃ compression molded films treated with different gamma-radiation doses

Radiation dose (kGy)	Degree of swelling, q (%)	Gel fraction (wt%)
15	355 ± 78	15 ± 4
25	140 ± 20	33 ± 2
40	61 ± 12	51 ± 6

absorbed energy and \bar{M}_n the number average molecular weight of the polymer before treatment. It is assumed that chain-scission and cross-linking occur at random and in proportion to the radiation dose. Eq. (7) holds for polymers with random, monomodal molecular weight distributions whether or not main-chain fracture occurs simultaneously with cross-linking. A plot of $s + \sqrt{s}$ as a function of the reciprocal of the radiation dose is presented in Fig. 7.

The network formation for the gamma-irradiated poly(TMC) could be adequately described using the Charlesby-Pinner model. The intercept for the best straight line was 0.78. This value corresponds to the ratio of chain scission to cross-linking per radiation dose. Gel formation can only occur if this ratio is lower than 2 [35]. In the absence of air, cross-linking is the main reaction that occurs upon gamma-irradiation of poly(TMC).

Considering the determined ratio of chain scission density to cross-linking density per radiation dose, the maximum obtainable gel fraction $(1-s)_{\max}$ can be determined as follows [36]:

$$(1-s)_{\max} = \frac{1}{2} \left[1 - \frac{G(s)}{G(x)} + \left(1 + \frac{2G(s)}{G(x)} \right)^{1/2} \right] \quad (8)$$

According to this expression, the maximum attainable gel fraction is 73% for poly(TMC) irradiated under vacuum.

As previously observed for other polymer systems, the extent of cross-linking of poly(TMC) upon gamma-irradiation is affected by the presence of air [35] (Table 5). Poly(TMC) films were packed in nitrogen, in air and under vacuum and were irradiated with a 25 kGy standard radiation dose. The gel fraction was significantly lower for air-packed films than for poly(TMC) films packed and sterilized in nitrogen or vacuum. This indicates a lower extent of cross-linking, possibly due to an increase of oxidative chain scission.

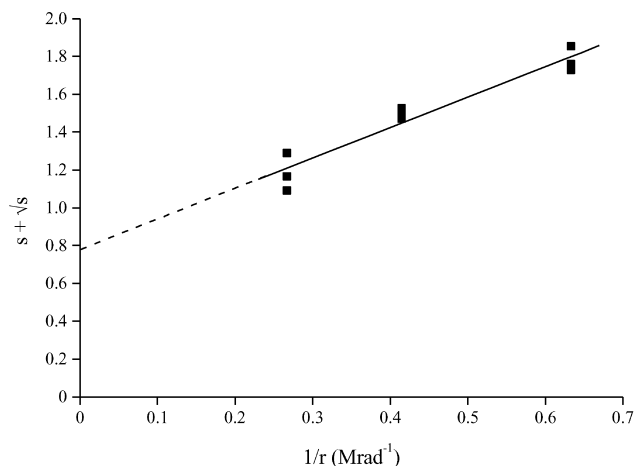


Fig. 7. Charlesby-Pinner plot for poly(TMC)₃ compression molded films ($\bar{M}_n = 208,000$ after processing) irradiated under vacuum. (1 kGy = 0.1 Mrad).

Table 5

Degree of swelling and gel fraction of poly(TMC)₅ compression molded films treated with a 25 kGy radiation dose under vacuum or in the presence of nitrogen or air

Packed under	Degree of swelling, q (%)	Gel fraction (wt%)
Vacuum	74 ± 2	54 ± 1
N ₂	73 ± 2	48 ± 2
Air	94 ± 5	28 ± 2

3.5. Mechanical properties of irradiated poly(TMC)

It is known that mechanical behavior of polymers can be improved by cross-linking [34,37]. However, as mentioned above, the cross-linking of poly(TMC) upon gamma-irradiation is accompanied by main chain-scissioning, which can lead to a reduction of elasticity modulus, tensile strength and creep resistance.

The tensile properties of high molecular weight poly(TMC) films irradiated in the absence of air with an average dose of 25 kGy are presented in Table 6.

At the standard sterilization dose of 25 kGy a slight decrease in the Young's modulus and stress at yield was found, compared to the results found for untreated samples (Table 6). In contrast, the strain at break had increased. This can be attributed to a plasticizing effect of lower molecular weight chains formed upon irradiation due to chain scission. Strain-induced crystallization was still observed, but the upturn in the stress-strain curves was found at higher strain values than for the non-irradiated samples (850% versus 500%). After the tensile test, the initially amorphous, irradiated poly(TMC) specimens ($T_g = -18^\circ\text{C}$) now showed a melting endotherm with a melting temperature (T_m) of 33°C ($\Delta H = 12\text{ J/g}$), confirming strain-induced crystallization of the polymer network. The lower heat of fusion reflects the lower degree of crystallinity attained by the cross-linked films upon straining which in turn accounts for the lower maximum tensile strength of the samples.

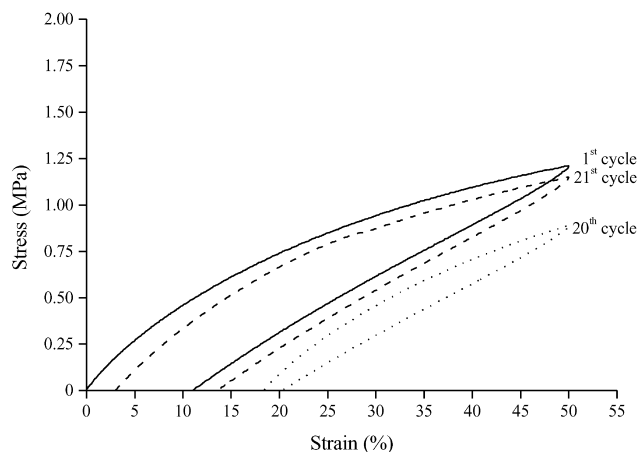


Fig. 8. Cyclic tensile test for high molecular weight poly(TMC)₃ compression molded films after gamma-irradiation treatment (25 kGy). Non-extracted films.

Table 6

Stress–strain behavior of poly(TMC)₄ compression molded films before and after gamma irradiation (25 kGy) under vacuum

Films	Young's modulus (MPa)	σ_{yield} (MPa)	ϵ_{yield} (%)	σ_{break} (MPa)	ϵ_{break} (%)	σ_{max} (MPa)
Untreated	6.6	2.1	120	15	890	16
Gamma-irradiated	5.0	1.5	150	9	1200	9

Non-extracted films.

Although the tensile properties of these samples decreased slightly upon gamma-irradiation, a great improvement was noticed in terms of the hysteresis effect. Tested under similar conditions as the non-treated samples, the irradiated compression-molded films showed better recovery 2 h after 20 consecutive deformation cycles (Fig. 8) as well as a much higher creep resistance (Table 7).

Poly(TMC) films irradiated in vacuum showed a permanent set of 3% after cyclic testing and subsequent recovery. The creep rates of these films decreased approximately two-fold in comparison with the non-irradiated films. The cross-links hinder the movement of polymer chains and reduce the viscous flow. The polymer becomes more elastic. As can be expected, the positive contribution of the covalent cross-links to the resistance of the polymer to creep increases with the extent of cross-linking. Samples irradiated in the presence of air showed higher creep rates than samples irradiated in the absence of air at the same stress applied (Table 7).

Presently, we are investigating the possibility of further improving the dimensional recovery of poly(TMC) upon mechanical deformation by irradiating the polymer with higher gamma-radiation doses and the effect of cross-linking upon gamma-irradiation on the in vivo degradation behavior of the polymer.

4. Conclusions

Very high molecular weight poly(TMC) (with \bar{M}_n above 200,000) shows rubber-like properties despite being totally amorphous and not cross-linked. In comparison to poly(TMC) of lower molecular weight it shows improved handling characteristics (lower tackiness), better dimensional stability and much improved mechanical behavior.

Table 7

Creep behavior of high molecular weight poly(TMC) after gamma-irradiation treatment (25 kGy) in the presence or absence of air. Non-extracted films

Applied stress (MPa)	Creep rate (s ⁻¹) (vacuum)	Creep rate (s ⁻¹) (air)
0.1 (5%) ^a	0.4×10^{-5}	0.9×10^{-5}
0.2 (10%)	1.2×10^{-5}	1.9×10^{-5}
0.4 (20%)	2.7×10^{-5}	8.8×10^{-5}
0.6 (30%)	6.5×10^{-5}	Not determined

Poly(TMC)₅ compression molded films.

^a The values in brackets correspond to approximate percentages of the yield stress in tensile tests performed on non-treated samples.

Very high molecular weight poly(TMC) is flexible and tough. The high maximum tensile strength of the polymer results from reinforcement of the structure upon strain-induced crystallization. These very high molecular weight rubbers show good recovery after mechanical deformation, considering that the only resistance to viscous flow comes from chain entanglement. A critical molecular weight (\bar{M}_n) below which the mechanical performance of the polymer is poor was determined to be 100,000. This is 40 times higher than the molecular weight between entanglements.

Gamma-irradiation of poly(TMC) results in simultaneous cross-linking and chain-scission. The ratio of scission density to cross-linking density per unit radiation dose was found to be 0.78. Upon irradiation of the polymer an insoluble network is formed, with increasing cross-linking density as the radiation dose is increased. The mechanical properties of very high molecular weight poly(TMC) rubbers improve upon irradiation. The irradiated polymer has significantly higher resistance to creep.

Acknowledgements

We acknowledge the PRAXIS XXI programme (Portuguese Foundation for Science and Technology) for financing this project (research grant BD/13335/97). We thank H. Kooster for carrying out the WAXS studies.

References

- [1] Buchholz B. *J Mater Sci: Mater Med* 1993;4:381–8.
- [2] Stock UA, Vacanti JP. *Annu Rev Med* 2001;52:443–51.
- [3] Wang Y, Ameer GA, Sheppard BJ, Langer R. *Nat Biotechnol* 2002; 20:602–6.
- [4] Sodergard A, Stolt M. *Prog Polym Sci* 2002;27:1123–63.
- [5] Grijpma DW, Zondervan GJ, Pennings AJ. *Polym Bull* 1991;25: 327–33.
- [6] Williams SF, Martin DP, Horowitz DM, Peoples OP. *Int J Biol Macromol* 1999;25:111–21.
- [7] Carothers WH, van Natta FJ. *J Am Chem Soc* 1930;52:314–26.
- [8] Engelberg I, Kohn J. *Biomaterials* 1991;12:292–304.
- [9] Katz AR, Mukherjee DP, Kaganov AL, Gordon S. *Surg Gynecol Obstet* 1985;161:213–22.
- [10] Grijpma DW, van Hofslot RDA, Super H, Nijenhuis AJ, Pennings AJ. *Polym Engng Sci* 1994;34:1674–84.
- [11] Jie C, Zhu KJ, Shilin Y. *Polym Int* 1996;41:369–75.
- [12] Jie C, Zhu KJ. *Polym Int* 1997;42:373–9.
- [13] Edlund U, Albertsson AC. *J Appl Polym Sci* 1999;72:227–39.
- [14] Pêgo AP, Poot AA, Grijpma DW, Feijen J. *J Biomater Sci Polym Ed* 2001;12:35–53.

- [15] Queslel JP, Mark JE. In: Mark HF, Bikales NM, Overberger CG, Menges G, Kroschwitz JI, editors. *Elasticity*, 2nd ed. Encyclopedia of polymer science and engineering, 5. New York: Wiley-Interscience; 1986. p. 365–408.
- [16] Pêgo AP, van Luyn MJA, Brouwer LA, van Wachem PB, Poot AA, Grijpma DW, Feijen J. *J Biomed Mater Res*, accepted for publication.
- [17] Wu S. *J Polym Sci Polym Phys* 1989;27:723–41.
- [18] Ferry JD. *Viscoelastic properties of polymers*, New York: Wiley; 1970.
- [19] Lide DR, editor. *CRC handbook of chemistry and physics*. Boca Raton, FL: CRC Press; 2002.
- [20] Zhu KJ, Hendren RW, Jensen K, Pitt CG. *Macromolecules* 1991;24: 1736–40.
- [21] Kowalski A, Duda A, Penczek S. *Macromol Rapid Commun* 1998;19: 567–72.
- [22] Pêgo AP, Poot AA, Grijpma DW, Feijen J. *Macromol Biosci* 2002;2: 411–9.
- [23] Kavesh S, Schultz JM. *Polym Engng Sci* 1969;9:452–60.
- [24] Crescenzi V, Manzini G, Calzolari G, Borri C. *Eur Polym J* 1972;8: 449–63.
- [25] Gent AN, Thomas AG. *J Polym Sci A2* 1972;10:571–3.
- [26] Flory PJ. *J Am Chem Soc* 1945;67:2048–50.
- [27] Turner DT. *Polymer* 1982;23:626–9.
- [28] Grijpma DW, Penning JP, Pennings AJ. *Colloid Polym Sci* 1994;272: 1068–81.
- [29] Morbitzer L, Hespe H. *J Appl Polym Sci* 1972;16:2697–708.
- [30] Kowalski JB, Morrissey RF. Sterilization of implants. In: Ratner BD, Hoffman AS, Schoen FJ, Lemons JE, editors. *Biomaterials science. An introduction to materials in medicine*. San Diego, CA: Academic Press; 1996. p. 415–20.
- [31] Edlund U, Albertsson AC, Singh SK, Fogelberg I, Lundgren BO. *Biomaterials* 2000;21:945–55.
- [32] Gilding DK, Reed AM. *Polymer* 1979;20:1459–64.
- [33] Birkinshaw C, Buggy M, Henn GG, Jones E. *Polym Degrad Stabil* 1992;38:249–53.
- [34] Darwis D, Mitomo H, Enjoji T, Yoshii F, Makuuchi K. *J Appl Polym Sci* 1998;68:581–8.
- [35] Charlesby A, Pinner SH. *Proc Roy Soc London* 1959;A249:367–86.
- [36] Inokuti M. *J Chem Phys* 1963;38:2999–3005.
- [37] Penning JP, Pras HE, Pennings AJ. *Colloid Polym Sci* 1994;272: 664–76.